

(Short Communication)

Large Signal Analysis of Low-Voltage BiMOS Analog Multipliers Using Fourier-Series Approximations

MUHAMMAD TAHER ABUELMA'ATTI

King Fahd University of Petroleum and Minerals
 Dhahran, Saudi Arabia

(Received September 30, 1999; Accepted January 17, 2000)

ABSTRACT

This paper discusses the large signal performance of BiMOS low-voltage analog multipliers. Fourier-series approximations are obtained for the transfer characteristics of the basic building blocks, such as the BiMOS folded Gilbert multiplier cell, the squaring multiplier made from two cross-coupled emitter-coupled pairs and driven by an MOS quadritail, and the tripler made from cross-coupled emitter-coupled pairs and driven by an MOS quarter-square multiplier. Using the Fourier-series approximations of the transfer functions of these basic building blocks, closed-form expressions are obtained for the amplitudes of the harmonics and intermodulation products at the output of these analog multipliers when excited by multisinusoidal input signals. Using these expressions, comparison between the large signal performance of these analog multipliers can be made and the parameters required for a predetermined performance can be determined.

Key Words: analog multipliers, BiMOS circuits, Fourier-series approximations, cross-coupled emitter-coupled pairs

I. Introduction

At present there is growing interest in designing low-voltage analog functional elements using the BiMOS technology. Because of their wide spread use in analog applications, multipliers are among the many functional circuits which can be realized using this technology.

With all the bipolar transistors assumed identical and their basewidth modulation ignored, and with all the MOS transistors assumed identical and operating in the saturation region and ignoring their body effect and channel-length modulation, the use of the square-law model for MOS transistors yields the expression of Eq. (1) for the differential output current of the BiMOS folded Gilbert multiplier cell, shown in Fig. 1 (Kimura, 1994).

$$y = f(z) \tanh(x), \quad (1a)$$

where

$$f(z) = z\sqrt{2-z^2}; \quad |z| \leq 1, \quad (1b)$$

$$f(z) = \operatorname{sgnz}; \quad |z| \geq 1, \quad (1c)$$

where $y = \Delta I_{out}/I_o \alpha_{Fp}$, $x = V_1/2V_T$, $z = V_2/\sqrt{I_o \beta}$, α_{Fp} is the dc common-base current gain factor for a pnp transistor, $V_T = kT/q$ is the thermal voltage, k is the Boltzman's con-

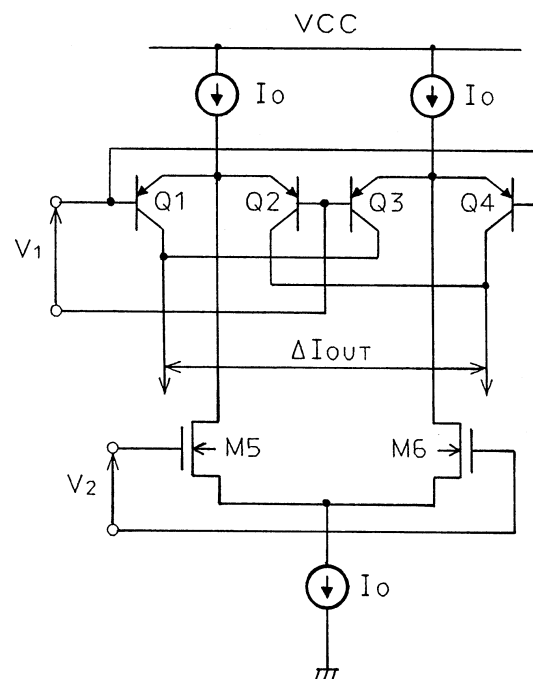


Fig. 1. BiMOS folded Gilbert multiplier cell.

stant, T is the absolute temperature in degrees Kelvin, q is the charge of an electron, $\beta = \mu C_{ox}/2(W/L)$ is the transcon-

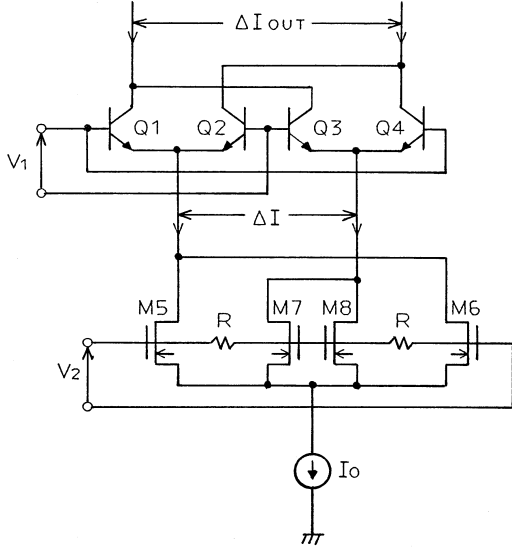


Fig. 2. Cross-coupled, emitter-coupled pairs driven by a MOS quadritail cell.

ductance parameter of the MOS transistor with effective surface mobility μ and gate capacitance per unit area C_{ox} , W is the gate width, and L is the gate length. Also, the differential output current of the cross-coupled emitter-coupled pairs driven by an MOS quadritail cell, as shown in Fig. 2, can be expressed as follows (Kimura, 1994):

$$y = g(z) \tanh(x), \quad (2a)$$

where

$$g(z) = \frac{1}{2} z^2; \quad |z| \leq \sqrt{\frac{2}{3}}, \quad (2b)$$

$$g(z) = \frac{1}{9} (z^2 - 3 + 2|z|\sqrt{2(6-z^2)}); \quad \sqrt{\frac{2}{3}} \leq |z| \leq 2, \quad (2c)$$

$$g(z) = 1; \quad |z| \geq 2, \quad (2d)$$

where $y = \Delta I_{out} / (\alpha_{Fn} I_o)$, α_{Fn} is the dc common-base current gain factor for an npn transistor. Finally, the differential output current of the cross-coupled emitter-coupled pairs driven by a MOS quarter-square cell, as shown in Fig. 3, can be expressed as follows (Kimura, 1995):

$$y = h(z, p) \tanh(x), \quad (3a)$$

$$h(z, p) = 2zp; \quad z^2 + p^2 + |zp| < \frac{1}{2}, \quad (3b)$$

$$h(z, p) = \frac{1}{9} (12zp - (3 + (|z| + |p|)^2 - 4(|z| - |p|)^2));$$

$$\cdot \sqrt{3 - 2(|z| + |p|)^2 + 6(|z||p|) \operatorname{sgn}(zp)});$$

$$z^2 + p^2 + |zp| \geq \frac{1}{2} \geq z^2 + p^2 - \frac{5}{3}|zp| \quad (3c)$$

$$h(z, p) = p\sqrt{1-p^2} \operatorname{sgn}(z) \tanh(x); \quad z^2 + p^2 - \frac{5}{3}|zp| \geq \frac{1}{2}, \quad (3d)$$

where $p = V_3 / \sqrt{I_o / \beta}$. Under small signal conditions, with the three normalized input voltages x , z and p restricted, respectively, to $x < 1/2$, $z < 1/2$ and $p < 1/2$, Eqs. (1) – (3) can be approximated, using the first term of the Taylor-series expansion of the tanh and square-root functions, by

$$y \cong \sqrt{2}xz, \quad (4)$$

$$y \cong \frac{1}{2}xz^2 \quad (5)$$

and

$$y \cong 2xzp. \quad (6)$$

Equations (4) – (6) show that, under small signal conditions, the three multipliers in Figs. 1 – 3 will perform the required multiplication. However, in their present forms, Eqs. (1) – (3) can not be used to predict the performance of the three multipliers under large signal conditions. This can be attributed, largely, to the lack of a single continuous function describing the transfer function of the multiplier and stretching over the useful range of its operation, in addition to the involvement of the tanh and square-root functions. Consequently, the tolerable nonlinearity and the dynamic range of the three multipliers can not be analytically defined.

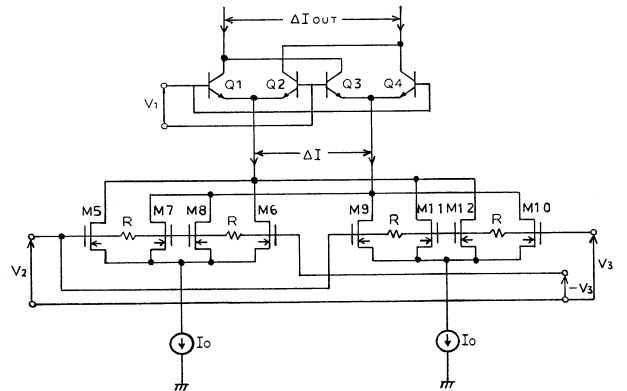


Fig. 3. Cross-coupled, emitter-coupled pairs driven by a MOS quarter-square multiplier.

The main objective of this paper is, therefore, to present a general analysis for predicting the nonlinear performance of BiMOS multipliers under large signal conditions. Using accurate models for the differential output current transfer functions, closed-form expressions are obtained for the amplitudes of the output products from a BiMOS multiplier with large-amplitude sinusoidal input signals. Using these expressions, a comparison between the different BiMOS multipliers can be made, and the optimum parameters required to meet a predetermined level of circuit performance can be determined.

II. Fourier-Series Approximation

Here we propose to approximate the functions $\tanh(x)$, $f(z)$, $g(z)$ and $h(z,w)$ of the three multipliers in Figs. 1 – 3 using the Fourier-series model of Eq. (7):

$$f(\phi) = a_o + \sum_{n=1}^N \left(a_n \cos\left(\frac{n\pi}{B}\phi\right) + b_n \sin\left(\frac{n\pi}{B}\phi\right) \right) \quad (7)$$

$$\frac{-B}{2} \leq \phi \leq \frac{B}{2}.$$

Equation (7) implies that the function $f(\phi)$ can be represented by a Fourier-series in the variable ϕ with periodicity, equal to $2B$, chosen such that the working range of the variable ϕ is an appropriate segment around zero. The parameters a_o , a_n and b_n , $n = 1, 2, \dots, N$, can be obtained using the procedure described by Abuelma'atti (1993). Since, $\tanh(x)$, $f(z)$ and $h(z,p)$ are odd functions, $a_n = 0$, $n = 0, 1, 2, \dots, N$. Tables 1 and 2 show typical values of B ,

Table 1. Values of the Parameters B and b_n for the Functions $\tanh(x)$ and $f(z)$

b_{2n+1}	$\tanh(x)$ $B = 8.0$	$f(z)$ $B = 8.0$
b_1	1.19595	1.25214
b_3	0.25269	0.36397
b_5	0.07189	0.16284
b_7	0.02075	0.06998
b_9	0.00607	0.02159
b_{11}	0.00172	-0.00144
b_{13}	0.00053	-0.00907
b_{15}	0.00013	-0.00829
b_{17}	0.00006	-0.00425
b_{19}	0.00000	-0.00030
b_{21}	0.00001	0.00196
b_{23}	0.00000	0.00232
b_{25}	0.00000	0.00144
b_{27}	0.00000	0.00021
b_{29}	0.00000	-0.00067
b_{31}	0.00000	-0.00091
b_{33}	0.00000	-0.00062
b_{35}	0.00000	-0.00012

Note: $a_o = a_n = b_{2n} = 0$, $n = 1, 2, \dots, N$.

Table 2. Values of the Parameters B and b_n for the Function $h(z,p)$

b_{2n+1}	$h(z,p)$ $p = 0.1$ $B = 8.0$	$h(z,p)$ $p = 0.2$ $B = 8.0$	$h(z,p)$ $p = 0.3$ $B = 8.0$	$h(z,p)$ $p = 0.4$ $B = 8.0$
b_1	0.17729	0.351889	0.520936	0.681303
b_3	0.05312	0.105420	0.155803	0.202857
b_5	0.02536	0.050350	0.074256	0.096156
b_7	0.01223	0.024326	0.035919	0.046656
b_9	0.00476	0.009578	0.014425	0.019520
b_{11}	0.00050	0.001194	0.002372	0.004577
b_{13}	-0.00164	-0.002994	-0.003583	-0.002928
b_{15}	-0.00234	-0.004358	-0.005565	-0.005845
b_{17}	-0.00212	-0.003964	-0.005168	-0.006014
b_{19}	-0.00143	-0.002682	-0.003616	-0.004641
b_{21}	-0.00061	-0.001183	-0.001784	-0.002568
b_{23}	0.000095	0.0000824	-0.000223	-0.000470
b_{25}	0.000548	0.0008821	0.0008029	0.0010993
b_{27}	0.0007168	0.0011738	0.0012442	0.0017793
b_{29}	0.0006446	0.0010522	0.0011979	0.0015199
b_{31}	0.0004181	0.0006837	0.0008372	0.0006154
b_{33}	0.0001380	0.0002449	0.0003551	-0.000411
b_{35}	-0.000109	-0.000124	-0.000080	-0.0010403

Note: $a_o = a_n = b_{2n} = 0$, $n = 1, 2, \dots, N$.

a_n , b_n for the functions $\tanh(x)$, $f(z)$ and $h(z,p)$ in Eqs. (1) and (3). Since, $g(z)$ is an even function, $b_n = 0$, $n = 1, 2, \dots, N$. Table 3 shows typical values of the parameters a_o , a_n , $n = 1, 2, \dots, N$, for the function $g(z)$.

From Table 2, it appears that the parameters b_n , $n = 1, 3, 5, \dots$ of the function $h(z,p)$ are, themselves, functions of p . Variations of the parameters b_n , $n = 1, 3, 5, 7$, with p are almost linear and can, therefore, be approximated by

$$b_n(p) \cong \delta_n p, \quad (8)$$

where $\delta_1 = 1.7729$, $\delta_3 = 0.5312$, $\delta_5 = 0.2536$ and $\delta_7 = 0.1223$. The variations of the parameters b_n , $n > 7$ can, if required, be fitted to polynomials as functions of p .

Using the parameters listed in Tables 1 – 3, calculations were performed, and the results are shown in Figs. 4 – 7 together with the transfer functions of Eqs. (1) – (3). From Figs. 4 – 7, it appears that the approximation of Eq. (7) accurately represents the transfer functions in Eqs. (1) – (3) with a relative root-mean-square (RRMS) error of 0.00064 for the transfer function $\tanh(x)$; 0.00144 for the transfer function $f(z)$ in Eq. (1); 0.017 for the transfer function $g(z)$ in Eq. (2); and 0.0037 for the transfer function $f(z,p)$ in Eq. (3) with $p = 0.1$, 0.0018 with $p = 0.2$, 0.0019, with $p = 0.3$ and 0.0049 with $p = 0.4$.

III. Large Signal Analysis of the Multipliers

If a nonlinear device, with a transfer characteristic modelled by Eq. (7), is excited by a multisinusoidal input signal of the form

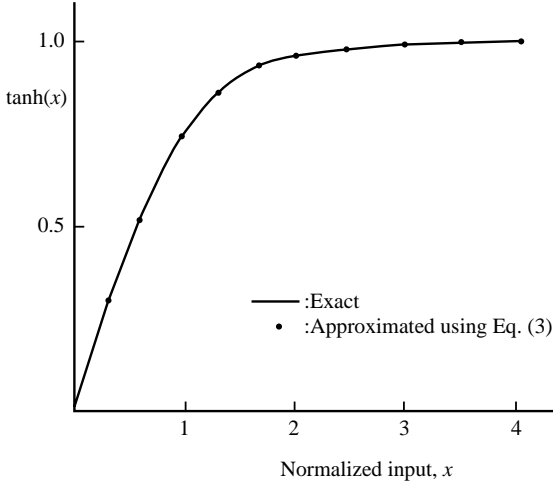


Fig. 4. The transfer function $\tanh(x)$. $\tanh(x)$ is an odd function.

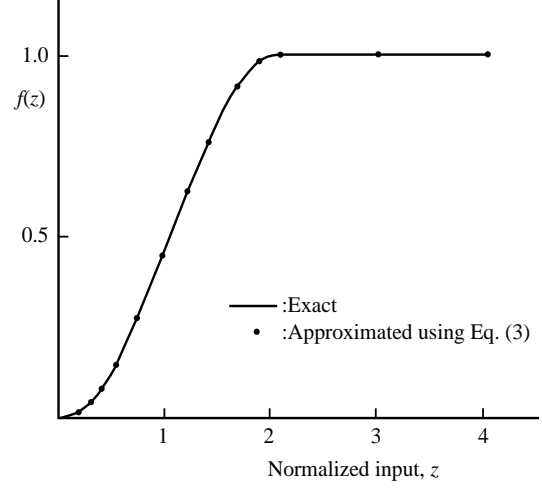


Fig. 6. The transfer function $g(z)$ in Eq. (2). $g(z)$ is an even function.

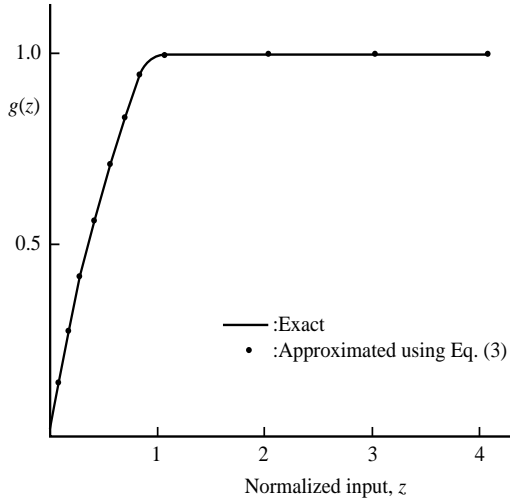


Fig. 5. The transfer function $f(z)$ in Eq. (1). $f(z)$ is an odd function.

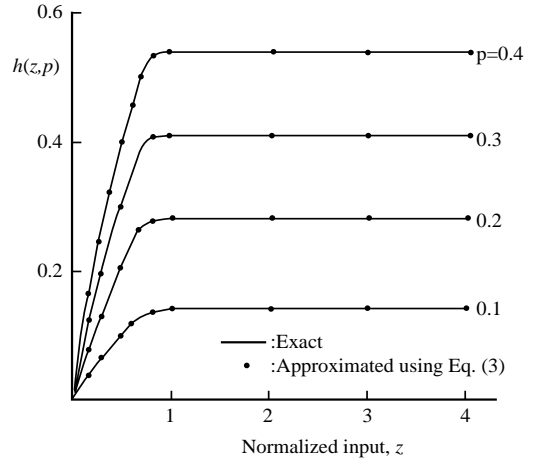


Fig. 7. The transfer function $h(z,p)$ in Eq. (3).

$$\phi(t) = \Phi_o + \sum_{k=1}^K \Phi_k \sin \omega_k t, \quad \Phi_o + \sum_{k=1}^K |\Phi_k| \leq \frac{B}{2}, \quad (9)$$

where Φ_o may represent an externally applied dc bias voltage, then by combining Eq. (7) with Eq. (9), the normalized output current can be obtained as

$$f(t) = a_o + \sum_{n=1}^N a_n \cos \left(\frac{n\pi}{B} \left(\Phi_o + \sum_{k=1}^K \Phi_k \sin \omega_k t \right) \right) + \sum_{n=1}^N b_n \sin \left(\frac{n\pi}{B} \left(\Phi_o + \sum_{k=1}^K \Phi_k \sin \omega_k t \right) \right). \quad (10)$$

Using the trigonometric identities:

$$\sin(\theta \sin \zeta) = 2 \sum_{l=0}^{\infty} J_{2l+1}(\theta) \sin(2l+1)\zeta,$$

$$\cos(\theta \sin \zeta) = J_0(\theta) + 2 \sum_{l=0}^{\infty} J_{2l}(\theta) \cos 2l\zeta,$$

it is easy to show that the amplitude of an output component of frequency $\sum_{k=1}^K \lambda_k \omega_k$, where λ_k is a positive or negative integer or zero, can be given by

$$F_{(\lambda_1, \lambda_2, \dots, \lambda_K)_c} = 2 \sum_{n=1}^N \left(a_n \cos \left(\frac{n\pi}{B} \Phi_o \right) + b_n \sin \left(\frac{n\pi}{B} \Phi_o \right) \right) \cdot \prod_{k=1}^K J_{|\lambda_k|} \left(\frac{n\pi}{B} \Phi_k \right) \quad \text{for } \sum_{k=1}^K |\lambda_k| = \text{even} \quad (11a)$$

and

$$F_{(\lambda_1, \lambda_2, \dots, \lambda_K)_s} = 2 \sum_{n=1}^N \left(b_n \cos\left(\frac{n\pi}{B} \Phi_o\right) - a_n \sin\left(\frac{n\pi}{B} \Phi_o\right) \right) \cdot \prod_{k=1}^K J_{|\lambda_k|}\left(\frac{n\pi}{B} \Phi_k\right) \quad \text{for } \sum_{k=1}^K |\lambda_k| = \text{odd}, \quad (11b)$$

where $J_{|\lambda_k|}(\theta)$ is the Bessel function of order $|\lambda_k|$ and $\sum_{k=1}^K |\lambda_k|$ is the order of the normalized output current component. Therefore, the amplitude of a normalized output current component of frequency ω_p can be given by

$$F_1 = 2 \sum_{n=1}^N \left(b_n \cos\left(\frac{n\pi}{B} \Phi_o\right) - a_n \sin\left(\frac{n\pi}{B} \Phi_o\right) \right) \cdot J_1\left(\frac{n\pi}{B} \Phi_p\right) \prod_{\substack{k=1 \\ k \neq p}}^K J_o\left(\frac{n\pi}{B} \Phi_k\right), \quad (12)$$

the amplitude of a normalized output m th harmonic current component of frequency $m\omega_p$ can be given by

$$F_m = 2 \sum_{n=1}^N \left(a_n \cos\left(\frac{n\pi}{B} \Phi_o\right) + b_n \sin\left(\frac{n\pi}{B} \Phi_o\right) \right) \cdot J_m\left(\frac{n\pi}{B} \Phi_p\right) \prod_{\substack{k=1 \\ k \neq p}}^K J_o\left(\frac{n\pi}{B} \Phi_k\right) \quad \text{for } m = \text{even} \quad (13a)$$

and

$$F_m = 2 \sum_{n=1}^N \left(b_n \cos\left(\frac{n\pi}{B} \Phi_o\right) - a_n \sin\left(\frac{n\pi}{B} \Phi_o\right) \right) \cdot J_m\left(\frac{n\pi}{B} \Phi_p\right) \prod_{\substack{k=1 \\ k \neq p}}^K J_o\left(\frac{n\pi}{B} \Phi_k\right) \quad \text{for } m = \text{odd}, \quad (13b)$$

and the amplitude of an intermodulation product of frequency $r\omega_p - q\omega_s$ and order $r + q$ can be given by

$$F_{(r,q)} = 2 \sum_{n=1}^N \left(a_n \cos\left(\frac{n\pi}{B} \Phi_o\right) + b_n \sin\left(\frac{n\pi}{B} \Phi_o\right) \right) \cdot J_r\left(\frac{n\pi}{B} \Phi_r\right) J_q\left(\frac{n\pi}{B} \Phi_q\right) \prod_{\substack{k=1 \\ k \neq r,q}}^K J_o\left(\frac{n\pi}{B} \Phi_k\right) \quad \text{for } r + q = \text{even} \quad (14a)$$

or

$$F_{(r,q)} = 2 \sum_{n=1}^N \left(b_n \cos\left(\frac{n\pi}{B} \Phi_o\right) - a_n \sin\left(\frac{n\pi}{B} \Phi_o\right) \right) \cdot J_r\left(\frac{n\pi}{B} \Phi_r\right) J_q\left(\frac{n\pi}{B} \Phi_q\right) \prod_{\substack{k=1 \\ k \neq r,q}}^K J_o\left(\frac{n\pi}{B} \Phi_k\right) \quad \text{for } r + q = \text{add}. \quad (14b)$$

In a similar way, the amplitude of an intermodulation product of any order can be obtained using Eq. (11).

From Eqs. (13) and (14), one can see that the amplitudes of odd-order products can be minimized through proper selection of the parameter Φ_o . Thus, proper selection of the dc bias voltage can yield minimum values of the amplitudes of the odd-order products.

Now if the input to the multiplier shown in Fig. 1 is composed of the two normalized signals

$$x(t) = X \sin \omega_1 t \quad (15)$$

and

$$z(t) = Z \sin \omega_2 t, \quad (16)$$

then, using Eq. (14b), the amplitude of the normalized output current of frequency $\omega_1 \pm \omega_2$ can be expressed as

$$Y_{\omega_1 \pm \omega_2} = 2 \sum_{n=1}^N b_n J_1\left(\frac{n\pi}{B} X\right) \sum_{m=1}^M b_{mf} J_1\left(\frac{m\pi}{B} Z\right), \quad (17)$$

where the subscript f means the parameters b_m of the function $f(z)$.

For sufficiently small values of X and Z such that $(N\pi/B)X \ll 1$ and $(M\pi/B)Z \ll 1$, the Bessel functions $J_1((n\pi/B)X)$ and $J_1((m\pi/B)Z)$ can be approximated by the first term of their Taylor series, that is, $J_1(\phi) \cong \phi/2$, and Eq. (17) reduces to

$$Y_{\omega_1 \pm \omega_2} \cong \frac{1}{2} \left(\frac{\pi}{B}\right)^2 \left(\sum_{n=1}^N n b_n\right) \left(\sum_{m=1}^M m b_{mf}\right) XZ. \quad (18)$$

From Table 1, we get $\sum_{n=1}^N n b_n = 2.54219$ and $\sum_{m=1}^M n b_{mf} = 3.57058$; thus, Eq. (18) can be reduced to

$$Y_{\omega_1 \pm \omega_2} \cong 0.699 XZ. \quad (19)$$

This is in excellent agreement with $0.707 XZ$, obtainable from Eq. (4).

In a similar way, the amplitude of the normalized

output current component of frequency $\omega_1 \pm 2\omega_2$ at the output of the multiplier shown in Fig. 2 can be expressed as

$$Y_{\omega_1 \pm 2\omega_2} = 2 \sum_{n=1}^N b_n J_1\left(\frac{n\pi}{B} X\right) \sum_{m=1}^M a_{2mg} J_2\left(\frac{m\pi}{B} Z\right), \quad (20)$$

where the subscript g means the parameters a_{2m} of the function $g(z)$. For sufficiently small values of X and Z such that $(M\pi/B)Z \ll 1$, the Bessel function $J_2((m\pi/B)Z)$ can be approximated by the first term of its Taylor series, that is, $J_2(\phi) \cong \phi^2/8$, and Eq. (20) reduces to

$$Y_{\omega_1 \pm 2\omega_2} \cong \frac{1}{8} \left(\frac{\pi}{B}\right)^3 \left(\sum_{n=1}^N nb_n\right) \left(\sum_{m=1}^M m^2 a_{mg}\right) XZ^2. \quad (21)$$

From Tables 1 and 3, we get $\sum_{n=1}^N nb_n = 2.54219$ and $\sum_{m=1}^M m^2 a_m = -6.10129$; thus, Eq. (21) reduces to

$$Y_{\omega_1 \pm 2\omega_2} \cong 0.117XZ^2. \quad (22)$$

This is in excellent agreement with $0.125XZ^2$, obtainable from Eq. (5).

Finally, the amplitude of the normalized output current component of frequency $\omega_1 \pm \omega_2$ at the output of the multiplier shown in Fig. 3 can be expressed as

$$Y_{\omega_1 \pm \omega_2} = 2 \sum_{n=1}^N b_n J_1\left(\frac{n\pi}{B} X\right) \sum_{m=1}^M b_{mh} J_2\left(\frac{m\pi}{B} Z\right), \quad (23)$$

where the subscript h means the parameters b_m of the function $h(z,p)$. In this case, the parameters b_{mh} are themselves functions of the third input $p(t)$. Thus, if the third input $p(t)$ can be expressed as

$$p(t) = P \sin \omega_3 t, \quad (24)$$

then, combining Eqs. (8), (23) and (24), the normalized output current component of frequency $\omega_1 \pm \omega_2 \pm \omega_3$ at the output of the multiplier shown in Fig. 3 can be expressed as

$$Y_{\omega_1 \pm \omega_2 \pm \omega_3} = P \left(\sum_{n=1}^N b_n J_1\left(\frac{n\pi}{B} X\right) \right) \sum_{m=1}^M \left(\delta_m J_1\left(\frac{m\pi}{B} Z\right) \right). \quad (25)$$

For sufficiently small values of X , Z , Eq. (25) reduces to

$$Y_{\omega_1 \pm \omega_2 \pm \omega_3} \cong \frac{1}{4} \left(\frac{\pi}{B}\right)^2 \left(\sum_{n=1}^N nb_n\right) \left(\sum_{m=1}^M m \delta_m\right) XZP. \quad (26)$$

From Tables 1 and 2, we get $\sum_{n=1}^N nb_n = 2.54219$ and $\sum_{m=1}^M m \delta_m = 5.36$; thus, Eq. (26) reduces to

$$Y_{\omega_1 \pm \omega_2 \pm \omega_3} \cong 0.5248XZP. \quad (27)$$

This is in excellent agreement with $0.5XZP$, obtainable from Eq. (6).

IV. Simulation Results

The multiplier circuits shown in Figs. 1 and 2 were

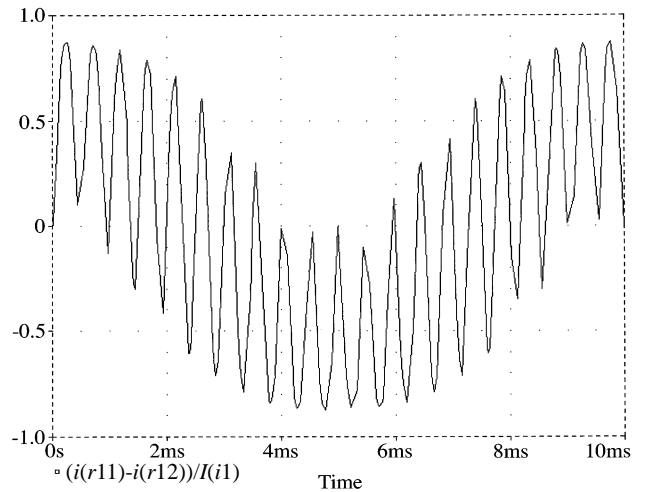


Fig. 8. Normalized output waveform obtained from Fig. 1 with $V_1 = 70$ mV, $V_2 = 1.4$ V, $f_1 = 1.1$ kHz and $f_2 = 1.0$ kHz.

Table 3. Values of the Parameters B and a_n , a_n for the Function $g(z)$

a_{2n}	$g(z)$
	$B = 8.0$ $a_0 = 0.74158$
a_2	-0.435104
a_4	-0.248765
a_6	-0.077377
a_8	0.0051283
a_{10}	0.0129087
a_{12}	0.0004342
a_{14}	-0.001357
a_{16}	0.0031416
a_{18}	0.0029340
a_{20}	-0.000751
a_{22}	-0.001876
a_{24}	-0.000343
a_{26}	0.0003589
a_{28}	-0.000298
a_{30}	-0.000421
a_{32}	0.0002816
a_{34}	0.0005344
a_{36}	0.0000809

Note: $a_{2n+1} = b_n = 0$, $n = 0, 1, 2, \dots, N$.

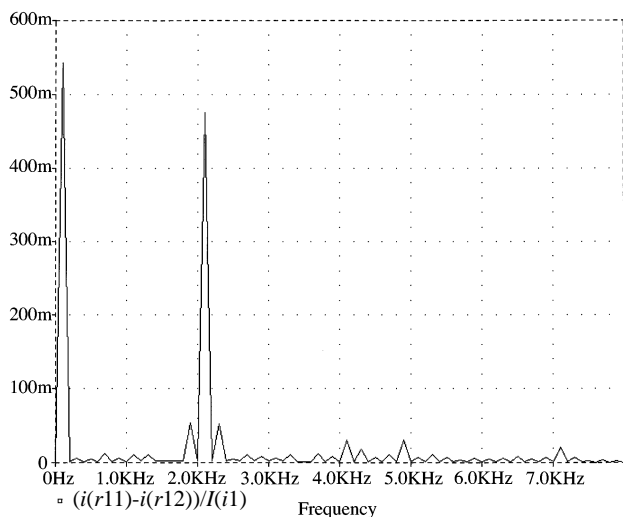


Fig. 9. Frequency spectrum of the waveform shown in Fig. 8.

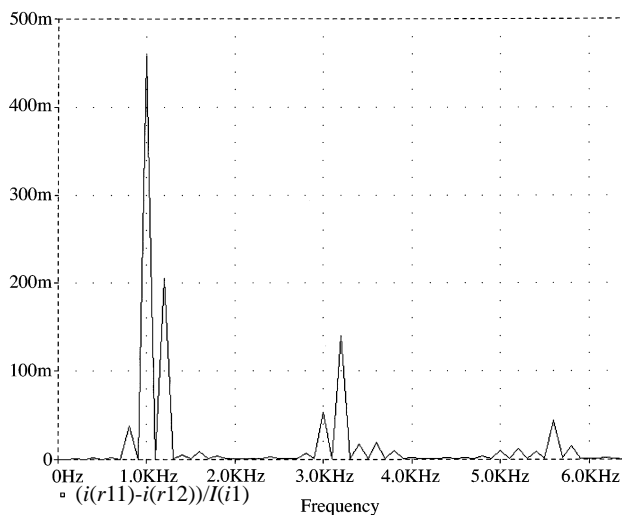


Fig. 11. Frequency spectrum of the waveform shown in Fig. 10.

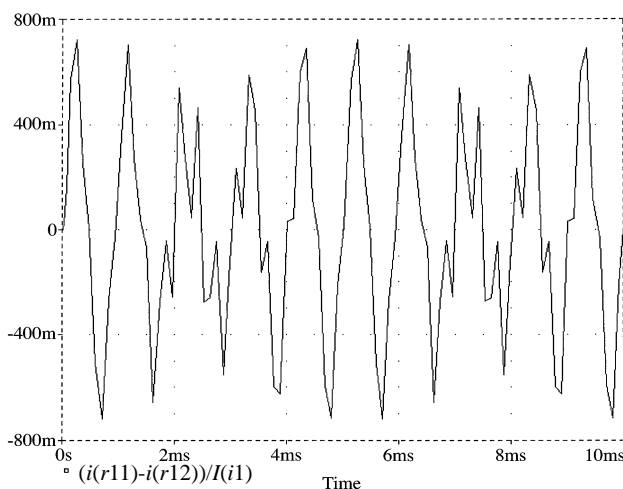


Fig. 10. Normalized output waveform obtained from Fig. 2 with $V_1 = 100$ mV, $V_2 = 2.0$ V, $f_1 = 1.1$ kHz and $f_2 = 1.0$ kHz.

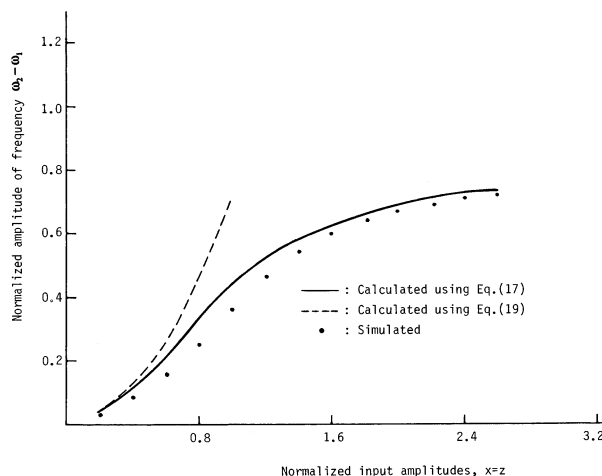


Fig. 12. Calculated and simulated results obtained using the multiplier shown in Fig. 1.

simulated using the evaluation version of the PSPICE circuit-simulation program. The parameters used were $I_s = 14$ fA, $\beta_f = 100$ and $V_{Af} = 100$ V for the npn and the pnp transistors, and $V_{To} = 2$ V, $K_p = 1$ mA/V² and $\gamma = 0.3$ V^{1/2} for the NMOS transistors. The supply voltage $V_{CC} = 5$ V, the current $I_o = 1$ mA, and the individual load resistor $R_L = 1$ k Ω . The results obtained are shown in Figs. 8 – 14.

Figure 8 shows a typical output waveform obtained from the multiplier circuit shown in Fig. 1 with $\omega_1 = 2200$ π rad/sec, $\omega_2 = 2000$ π rad/sec and $X = Z = 1.4$, which corresponds to $V_1 = 70$ mV and $V_2 = 1.4$ V. Figure 9 shows the frequency spectrum of the output waveform shown in Fig. 8.

Figure 10 shows a typical output waveform obtained from the multiplier circuit shown in Fig. 2 with $\omega_1 = 2200$

π rad/sec, $\omega_2 = 2000$ π rad/sec and $X = Z = 2.0$, which corresponds to $V_1 = 100$ mV and $V_2 = 2.0$ V. Figure 11 shows the frequency spectrum of the output waveform shown in Fig. 10.

It appears from Figs. 8 – 11 that the multiplier circuits shown in Figs. 1 and 2 can successfully perform multiplication under relatively large signals, and that their operation is not limited to small signals as mentioned by Kimura (1994).

Figures 12 – 14 show the variation of the normalized output amplitudes with the normalized inputs. Also shown are the calculated results obtained using Eqs. (17) and (19) for the multiplier circuit shown in Fig. 1, using Eqs. (20) and (22) for the multiplier circuit shown in Fig. 2 and using Eqs. (25) and (27) for the multiplier circuit shown in

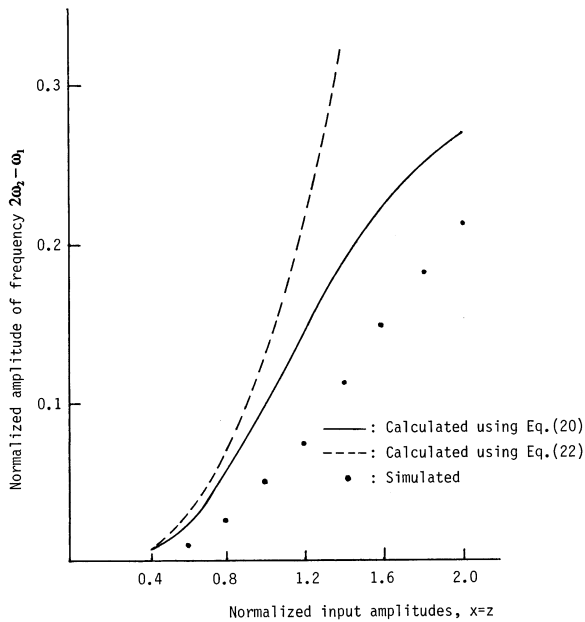


Fig. 13. Calculated and simulated results obtained using the multiplier shown in Fig. 2.

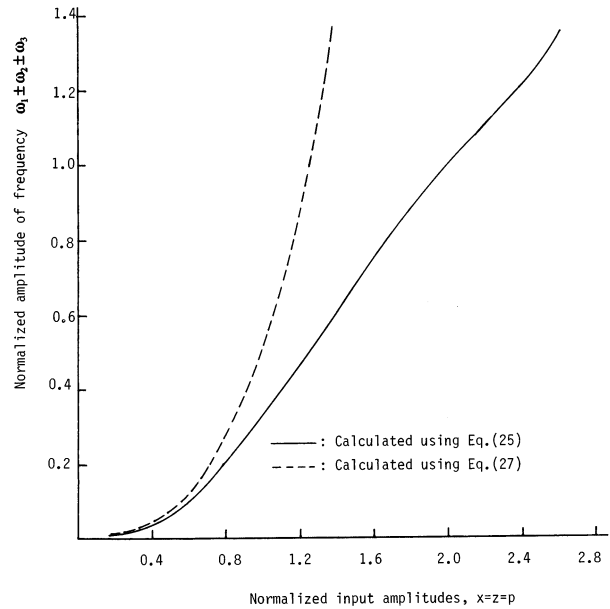


Fig. 14. Calculated results obtained using the multiplier shown in Fig. 3.

Fig. 3.

From Figs. 12 and 13 it appears that the simulation results are in fairly good agreement with the calculated results obtained using the theory presented here. Also, it appears from Figs. 12 – 14 that Eqs. (19), (22) and (27) can be used to predict the multiplier performance accurately for values of $X = Z = P < 0.4$.

V. Conclusion

This paper has presented large signal analysis for the BiMOS low-voltage analog multiplier circuits. By approximating the nonlinear transfer characteristics of the basic building blocks, such as the folded Gilbert multiplier cell, the squaring multiplier made from two cross-coupled emitter-coupled pairs and driven by a MOS quadritail, and the tripler made from cross-coupled emitter-coupled pairs and driven by a MOS quarter-square multiplier, the output spectrum of the analog multipliers can be obtained. In general, the spectrum computation performed using these expressions requires the use of the ordinary Bessel func-

tions. In contrast with the comments made by Kimura (1994), the results obtained in this paper clearly show that these BiMOS analog multipliers can be successfully used for large signal as well as small signal multiplication.

It is worth mentioning here that the results presented in this paper were obtained based on the assumption that the basic building blocks are memoryless. This may be a reasonable assumption at relatively low frequencies. At high frequencies, however, the parasitic effects of the transistors must be taken into consideration. This will result in frequency-dependent nonlinear transfer characteristics.

References

- Abuelma'atti, M. T. (1993) A simple algorithm for fitting measured data to Fourier-series models. *International Journal of Mathematical Education in Science and Technology*, **24**, 107-112.
- Kimura, K. (1994) Some circuit design techniques using two cross-coupled, emitter-coupled pairs. *IEEE Transactions on Circuits and Systems-I: Fundamental Theory and Applications*, **41**, 411-423.
- Kimura, K. (1995) Circuit design techniques for very low-voltage analog functional blocks using triple-tail cells. *IEEE Transactions on Circuits and Systems-I: Fundamental Theory and Applications*, **42**, 873-885.

M.T. Abuelma'atti

低電壓 BiMOS 類比乘法器利用傅立葉級數近似法之大訊號分析

MUHAMMAD TAHER ABUELMA'ATTI

*King Fahd University of Petroleum and Minerals
Dhahran, Saudi Arabia*

摘 要

本論文討論 BiMOS 低電壓類比乘法器之大訊號性能。基本建構方塊電路，例如 BiMOS 摺疊式 Gilbert 乘法器，用兩個射極互藕及一個 MOS 四級尾端做成的平方乘法器，以及用射極互藕和一個 MOS 四等分/平方之三次方乘法器的轉移函數的傅立葉級數近似可被推導出來。利用這些基本方塊電路的轉移函數的傅立葉函數近似可以得到當這些乘法器的輸入為多重頻率之正弦波時，其輸出端的諧波振幅和交互調變乘積的封閉式表示式。利用這些表示式，可以比較出各種類比乘法器的大訊號表現，同時可以決定預設表現下的參數值。